# Vorticity and magnetic shielding in a type-II superconductor

**Marco Cardoso, Pedro Bicudo and Pedro D Sacramento**

Departamento de Física and CFIF, Instituto Superior Técnico, Av. Rovisco Pais, 1049-001 Lisboa, Portugal

**Abstract**

We study in detail, solving the Bogoliubov–de Gennes equations, the magnetic field, supercurrent and order parameter profiles originated by a solenoid or magnetic whisker inserted in a type-II superconductor. We consider solutions of different vorticities, $n$, in the various cases. The results confirm the connection between the vorticity, the internal currents and the boundstates in a self-consistent way. The number of boundstates is given by the vorticity of the phase of the gap function as in the case with no external solenoid. In the limiting case of an infinitely thin solenoid, like a Dirac string, the solution is qualitatively different. The quasiparticle spectrum and wavefunctions are a function of $n - n_{\text{ext}}$, where $n_{\text{ext}}$ is the vorticity of the solenoid. The flux is in all cases determined by the vorticity of the gap function.

(Some figures in this article are in colour only in the electronic version)

## 1. Introduction

The effect of a magnetic field on a superconductor has attracted interest for a long time. At small fields the superconductor is rigid to the external field but for a sufficiently strong field, or a high enough electric current flowing through the material, superconductivity is destroyed. In type-II superconductors there is a low critical field, $H_{c1}$, above which the field lines penetrate the superconductor in the form of quantized vortex lines. As the field increases, the vortex line density also increases until the vortex cores overlap and the system becomes non-superconducting at the high critical field, $H_{c2}$. The external field is shielded by the appearance of compensating currents that cancel the external field beyond a penetration length, $\lambda$. Another length which is important is the coherence length, $\zeta$, which measures the range of the establishment of the superconducting order parameter into the superconducting region. Since many important superconductors, like the high-$T_c$ materials, are strong type-II superconductors, the presence of external magnetic fields implies proliferation of vortices and, therefore, their influence has been thoroughly studied.

In this work we consider the effects of a vortex induced by the insertion of a long solenoid or magnetic whisker of very small width in the superconductor. Due to recent technological advances it is possible to construct magnetic systems of nano size of the order of the coherence length or penetration length. We consider that the inserted foreign system is long enough so that the field lines penetrate the material (eventually through the effect of the vector potential) but that the field lines return far from the superconducting film, such that no antivortices are created inside the material. Solving the Bogoliubov–de Gennes equations we study in detail the energy spectra and its consequences on the physical properties due to the presence of the external solenoid, paying special attention to the magnetic shielding due to the Meissner effect.

The problem of the quasiparticle states due to the presence of a vortex in an s-wave superconductor was solved long ago both analytically [1] and numerically [2]. There are bound states localized in the vicinity of the vortex location and a continuum of delocalized states. The case of a d-wave superconductor led to some controversy but it was established that the states are delocalized, consistently with a gapless spectrum [3]. Classifying the states in terms of the angular momentum around the vortex line, allowed one to determine that there is a branch of boundstates, one for each angular momentum value [2]. The results were obtained looking for an order parameter of the form $\Delta = \Delta_0 e^{-in\varphi}$, where $\varphi$ is the polar angle and $n$ fixes the vorticity, chosen originally as $n = 1$. The core states are coherent superpositions of particle and hole states and are interpreted as being the result of constructive interference of multiple Andreev scattering from the spatial variation of the order parameter [4]. Also, it was shown that the main contribution to the supercurrent is originated in these states. At very low temperatures the quantum nature of the bound states gains importance and oscillations in the various quantities are quite pronounced [5]. The quantum limit is obtained when the thermal width is smaller than the level spacing and is reached when $T/T_c \leqslant 1/(k_F\zeta_0)$, where $T_c$ is the critical temperature, $k_F$ is the Fermi momentum and $\zeta_0 = \hbar v_F/\pi \Delta_0$ is the coherence length. In the typical type-II layered superconductor NbSe$_2$ the critical temperature is $T_c = 7.2$ K and $k_F\zeta_0 \sim 70$. The quantum limit is reached for rather low temperatures of the order of 50 mK, but for the high-temperature superconductors, where the critical temperature is high and the coherence length is small, the quantum limit is reached for temperatures of the order of 10 K. In this limit, Friedel-like oscillations are found in contrast to a Ginzburg–Landau description. In particular the Kramer–Pesch effect [6], in which the vortex core size increases with temperature, is not explainable in terms of normal electrons. The oscillations in the various quantities are observed at sufficiently low temperatures, irrespective of the size of $k_F\zeta_0$.

Even though as the field increases it is energetically favourable that many single vortices appear, as compared to fewer vortices with higher units of flux [7], the possibility of multi-flux vortices (or giant vortices) has been considered in particular systems and situations. In this case it has been predicted that there are $n$ branches of boundstates (where $n$ is the vorticity of the flux line) [8] and this has been confirmed by several authors [9]. If formed, the doubly quantized vortex is metastable against dissociation into singly quantized vortices. In this case a counter-circulating current appears in the core [4] which is due to a bound state that appears below the Fermi level. At high temperatures this state is depopulated, the current reversal disappears and this leads to a structure similar to the Ginzburg–Landau description. The appearance of $n$ discrete branches of states for a vortex with vorticity $n$ should be seen in scanning tunnelling microscopy (STM) measurements in the form of $n$ rows of peaks as a function of the distance from the vortex core [9]. Oscillations in the current due to the multiple vortices were observed at low temperatures in a form that is qualitatively different from results obtained from a Ginzburg–Landau description [10]. These oscillations are also observed in the order parameter.

Multiply quantized vortices have been observed in type-I superconductor films at high magnetic fields [11]. In high-temperature superconductors having columnar or large pointlike

defects acting as pinning centres, multiply quantized vortices may appear as well. Giant-vortex states have also been observed in superconductors with strong geometrical constraints, like in triangles or squares of sizes of the order of the $\mu$m, using a scanning SQUID microscope [12]. The possibility of different vorticities leads to interesting features like the Little Parks effect where oscillations of the critical temperature, as the external field changes, occur due to transitions between states with different vorticities [13].

In general, we may have a mixture of vortices with different winding numbers. Recently, in a NbSe$_2$ traditional superconductor, where normal metal islands of gold are inserted, a coexistence of strongly interacting multiquanta vortices distributed in a lattice with interstitial single vortices has been observed [14]. The case of a single normal dot inserted in a superconductor was also studied [15]. The dot is quite small of a subnanometre scale. It was found that the energy spectrum strongly depends on the number of flux quanta penetrating the dot and it was shown that the number of branches corresponds to the number of flux quanta. To guarantee that any vortices in the system would be in the dot, fields smaller than $H_{c1}$ were used. It was shown that by increasing the dot size the vorticity of the dot could be increased and therefore different states could be studied directly.

The vortex lines in general appear due to the application of an external magnetic field, typically homogeneous. However, we can also consider the presence of magnetic field lines that are due to a solenoid or a magnetic rod inserted in the superconductor. Actually, the magnetic field lines do not need to penetrate the superconductor itself, since what really matters is the vector potential. It is the vector potential that appears in the Hamiltonian of the system in the presence of a magnetic field [7], as is well known. This has been emphasized [16] considering a superconductor in the form of a cylindrical shell of internal radius $R$ and width $a$ in the centre of which is inserted either a solenoid or a magnetic rod of radius $r$ smaller than $R$. In these systems, considering the length of the cylinders to be very large compared to the radius, the field lines will close far from the superconductor and therefore no field lines penetrate the cylinder. However, the vector potential due to the flux contained in the transverse section is non-zero and the field has the same effect on the supercurrents.

We may also consider other situations in which there is an interplay between magnetic systems and superconductors. Recently the situation of ferromagnet–superconductor hybrid systems has been reviewed [17, 18]. On the one hand it has been proposed that we can manipulate spin and charge in magnetic semiconductors using superconducting vortices, with applications in spintronics [19]. On the other hand we may consider the effect of the magnetic system on the superconductor. The magnetic film is separated from the superconducting layer to avoid suppression of superconductivity by the proximity effect. This is attained by introducing a thin insulating layer between the two films.

A possibility to insert a magnetic field in the superconductor is through the field originated by a magnetic dot. Depending on the strength of the magnetization of the dot we may have single or multiple vortices. Using a London theory it has been found that giant vortices occur when the dot size is small enough [20], with a size of the order of $4.5\zeta$. Otherwise the energetically favourable situation is the presence of single quantized vortices [20]. Considering an array of magnetic dots, these originate vortices in the superconductor which are preferably bound to the magnetic dots in a way that is more advantageous than those due to the usual defect pinning centres [21]. In zero field the dots, which are far apart, are not coupled and are oriented randomly. Therefore any other vortices that may not be bound to the dots, or that appear as fluctuations, will feel the presence of a random magnetization and will be in a resistive state. However, if a field is applied the dots align, and if field cooled the film may be superconducting. The ordered commensurate state is then favoured. The pinning turns out to be more effective than with non-magnetic dots. Also, the critical current has the unusual property that it is

increased with field. Therefore, introducing magnetic nanoparticles or nanorods one obtains what are called frozen flux superconductors [22, 23]. In these systems a thermodynamically stable state of frozen flux lines is obtained showing that the magnetic dots are more effective than other pinning centres. This is important for controlling the maximum currents that may flow in the superconductor. Additional flux lines created by an applied magnetic field need to overcome big energy barriers in order to move. As mentioned above, larger systems were also considered such as two films, one magnetic and the other superconducting, close by [24]. In this close vicinity the magnetic field created by the supercurrents interacts with the magnetic subsystem. The interplay between the two systems leads to interesting magnetic structures like the cryptoferromagnetic state [25] and commensurability effects lead to an increase of critical current [26].

Since the total flux created by the magnetic dot is zero if the superconducting film is large enough, one may expect the presence of vortices and antivortices, due to the dipole field of the dot. In a type-II superconductor the interaction between two vortices is repulsive and the interaction between a vortex and an antivortex is attractive. In studies close to the critical line it has been found that the antivortices may coexist with the vortices, but away from the vicinity of the critical line they disappear. However, in type-I superconductors the interaction between a vortex and an antivortex is repulsive (and the interaction between two vortices is attractive). Therefore it is possible that structures with vortices and antivortices may appear in type-I systems. Also, small systems show confinement effects on the vortices: due to the strong increase of the kinetic energy term near the frontier, it is favourable for the system to be in the superconducting state close to the borders. Therefore it is not favourable for a vortex to approach the borders of the system. As a consequence they tend to be close together near the centre, particularly if the system size is very small. Considering a type-I system with a triangular symmetry, it has been shown that stable vortex–antivortex structures are indeed possible [27]. A rich variety of vortex structures has been studied recently [28].

All of these results show the importance of the study of complex structures of vortices and their interplay with magnetic structures. Recently it was stressed that the important characteristic that determines the boundstates is the winding of the phase [29]. The detailed form of the order parameter in the vicinity of the vortex core is not so relevant. Performing a non-self-consistent study of the spectrum, it was found that the suppression of the gap function has a minor role. The supercurrent acts in a non-symmetrical way on the particle and hole parts of the quasiparticles. It tends to decrease the angular momentum of the particle part and to increase the angular momentum of the hole part.

In this work we consider the same problem from a different point of view. We perform a self-consistent solution of the influence of a very long solenoid on the properties of the system. We consider different possible vorticities and study how the system responds to the external perturbation. The internal field must adjust itself to the solution chosen according to the external field exerted by the solenoid. The total magnetic flux is fully determined by the choice of the angular momentum of the gap function and the value of $n$ determines the vorticity of the vortex solution. This may be a single or a multiple vortex. Depending on the relation of the value of $n$ and the value of the external field, the internal currents will create fields that compensate, undercompensate or overcompensate the external field. The various situations lead to different spectral structures, depending on the width of the solenoid. These in turn originate different structures for the internal field and supercurrents generated. The limit of a very thin solenoid is qualitatively different. It is shown that when the vorticity chosen equals the unit of external flux the currents generated vanish and no bound states appear. Otherwise the currents may be positive, and branches of boundstates with positive energies appear or the currents are negative and branches of negative energies appear. These results confirm the link between the

boundstates and the internal currents in a self-consistent way. In the case of a finite width solenoid the number of boundstates equals the vorticity of the gap function and is insensitive to the external field. The results presented here may also describe a magnetic dot superimposed on the superconductor if in addition to the magnetic field due to the dot we apply an external homogeneous field. In this case the external field compensates the negative field lines due to the dot [17] that appear away from the dot position. We also consider the more complex and realistic case of a magnetic rod inserted in the superconductor.

## 2. Method

### 2.1. Bogoliubov–de Gennes equations

Consider the Bogoliubov–de Gennes (BdG) equations

$$
\begin{aligned}
\left[ \frac{1}{2m} \left( \mathbf{p} - \frac{e}{c}\mathbf{A} \right)^2 + U(\mathbf{r}) - E_{\mathrm{F}} \right] u_i(\mathbf{r}) + \Delta(\mathbf{r})v_i(\mathbf{r}) &= E_i u_i(\mathbf{r}) \\
-\left[ \frac{1}{2m} \left( \mathbf{p} + \frac{e}{c}\mathbf{A} \right)^2 + U(\mathbf{r}) - E_{\mathrm{F}} \right] v_i(\mathbf{r}) + \Delta^*(\mathbf{r})u_i(\mathbf{r}) &= E_i v_i(\mathbf{r})
\end{aligned}
\tag{1}
$$

where $U(\mathbf{r})$ is an external potential, $\mathbf{A}(\mathbf{r})$ is the vector potential, and where we consider s-wave pairing, for simplicity. $\Delta(\mathbf{r})$ is the pairing function given by

$$
\Delta(\mathbf{r}) = g \sum_{0 < E_i \leqslant \hbar\omega_D} u_i(\mathbf{r})v_i^*(\mathbf{r})[1 - 2f(E_i)].
\tag{2}
$$

Here $f(E_i)$ is the Fermi–Dirac distribution. The vector potential is given by Maxwell's equations:

$$
\nabla \times \mathbf{B} = \nabla \times \nabla \times \mathbf{A} = \frac{4\pi}{c}\mathbf{J}_{\mathrm{total}}
\tag{3}
$$

which, in the Coulomb gauge ($\nabla \cdot \mathbf{A} = 0$), is given by

$$
\nabla^2 \mathbf{A} = -\frac{4\pi}{c}\mathbf{J}_{\mathrm{total}}.
\tag{4}
$$

The current density originated in the supercurrents is obtained self-consistently by

$$
\begin{aligned}
\mathbf{J}(\mathbf{r}) = \frac{e\hbar}{\mathrm{i}m} \sum_i & f(E_i)u_i^*(\mathbf{r})\left[ \nabla - \frac{\mathrm{i}e}{\hbar c}\mathbf{A}(\mathbf{r}) \right] u_i(\mathbf{r}) \\
& + [1 - f(E_i)]v_i(\mathbf{r})\left[ \nabla - \frac{\mathrm{i}e}{\hbar c}\mathbf{A}(\mathbf{r}) \right] v_i^*(\mathbf{r}) - \mathrm{c.c.}
\end{aligned}
\tag{5}
$$

### 2.2. Diagonalization of the Hamiltonian

We assume no dependence along the axis of the vortex line ($z$-axis) and cylindrical symmetry both of the superconductor and of the potential $U(\mathbf{r})$. Let us take the order parameter in the form

$$
\Delta(\mathbf{r}) = \Delta(\rho)\mathrm{e}^{-\mathrm{i}n\varphi}.
\tag{6}
$$

This form describes a magnetic flux equal to $n$ flux quanta ($\Phi = n\Phi_0 = n\frac{hc}{2e}$).

The wavefunctions $u_i$ and $v_i$ are expanded in a way similar to reference [2]:

$$
u_i(\mathbf{r}) = \sum_{\mu, j} c_{\mu, j}^i \phi_{j, \mu-1/2}\mathrm{e}^{\mathrm{i}(\mu-1/2)\varphi}
\tag{7}
$$

$$
v_i(\mathbf{r}) = \sum_{\mu, j} d_{\mu, j}^i \phi_{j, \mu-1/2+n}\mathrm{e}^{\mathrm{i}(\mu-1/2+n)\varphi}
\tag{8}
$$

where the basis functions are

$$\phi_{jm}(\rho) = \frac{\sqrt{2}}{R J_{m+1}(\alpha_{jm})} J_m\left(\alpha_{jm}\frac{\rho}{R}\right).$$ (9)

The system is placed in a cylinder of radius $R$. Given the azimuthal symmetry of the system, neither $\Delta(\rho)$ nor $\mathbf{A}$ depend on $\varphi$. Therefore the Hamiltonian may be diagonalized separately for each value of the angular momentum $\mu$. The functions $J_m$ are the spherical Bessel functions and $\alpha_{jm}$ is the $j$th zero of the Bessel function of order $m$. The set of values of the angular momentum is given by $\mu = \pm(2l+1)/2$, where $l = 0, 1, 2, \ldots$. The terms $(\mu - 1/2)$ and $(\mu - 1/2 + n)$ may be rewritten in a more symmetrical way like $(\mu' - n/2)$ and $(\mu' + n/2)$ if $\mu'$ is half-odd integer if $n$ is odd and $\mu'$ is integer if $n$ is even.

For each eigenvalue $E_i$, we have a single value of $\mu$ and it is enough to diagonalize the matrix, defined in the subspace of the zeros of the Bessel function,

$$\begin{pmatrix} T^- & \Delta \\ \Delta^{\mathrm{T}} & T^+ \end{pmatrix} \begin{pmatrix} c_\mu^i \\ d_\mu^i \end{pmatrix} = E_i \begin{pmatrix} c_\mu^i \\ d_\mu^i \end{pmatrix}$$ (10)

where

$$T_{jj'}^- = \frac{\hbar^2}{2m}\frac{\alpha_{j,\mu-1/2}^2}{R^2}\delta_{jj'} - (\mu - 1/2)\frac{e}{\hbar c}I_1^- + \frac{e^2}{\hbar^2 c^2}I_2^- - E_{\mathrm{F}} + I_3^-$$ (11)

$$T_{jj'}^+ = -\frac{\hbar^2}{2m}\frac{\alpha_{j,\mu-1/2+n}^2}{R^2}\delta_{jj'} - (\mu - 1/2 + n)\frac{e}{\hbar c}I_1^+ - \frac{e^2}{\hbar^2 c^2}I_2^+ + E_{\mathrm{F}} - I_3^+$$ (12)

with

$$I_1^- = \int_0^R \phi_{j,\mu-1/2}(\rho)\frac{A_\varphi(\rho)}{\rho}\phi_{j',\mu-1/2}(\rho)\rho\,\mathrm{d}\rho$$ (13)

$$I_1^+ = \int_0^R \phi_{j,\mu-1/2+n}(\rho)\frac{A_\varphi(\rho)}{\rho}\phi_{j',\mu-1/2+n}(\rho)\rho\,\mathrm{d}\rho$$ (14)

and

$$I_2^- = \int_0^R \phi_{j,\mu-1/2}(\rho)A_\varphi(\rho)^2\phi_{j',\mu-1/2}(\rho)\rho\,\mathrm{d}\rho$$ (15)

$$I_2^+ = \int_0^R \phi_{j,\mu-1/2+n}(\rho)A_\varphi(\rho)^2\phi_{j',\mu-1/2+n}(\rho)\rho\,\mathrm{d}\rho$$ (16)

and

$$I_3^- = \int_0^R \phi_{j,\mu-1/2}(\rho)U(\rho)\phi_{j',\mu-1/2}(\rho)\rho\,\mathrm{d}\rho$$ (17)

$$I_3^+ = \int_0^R \phi_{j,\mu-1/2+n}(\rho)U(\rho)\phi_{j',\mu-1/2+n}(\rho)\rho\,\mathrm{d}\rho.$$ (18)

Also we have

$$\Delta_{jj'} = \int_0^R \phi_{j,\mu-1/2}(\rho)\Delta(\rho)\phi_{j',\mu-1/2+n}(\rho)\rho\,\mathrm{d}\rho.$$ (19)

It is important to note that the symmetry of the BdG equations

$$u_i(\mathbf{r}) \to v_i^*(\mathbf{r})$$ (20)

$$v_i(\mathbf{r}) \to -u_i^*(\mathbf{r})$$ (21)

$$E_i \to -E_i$$ (22)

allows us to reduce the solution to the positive values of $\mu$. We obtain the eigenvectors and eigenvalues for negative values of $\mu$ using the above symmetry.

## 2.3. Calculation of the vector potential

Consider a general situation where the total vector potential is given by the sum of an external potential and the internal vector potential originated on the supercurrents. Then we can write that

$$\vec{A} = \vec{A}_{\text{ext}} + \vec{a} \tag{23}$$

where $\vec{a}$ is the internal gauge potential. Then naturally we can write that

$$\Phi = \Phi_a + \Phi_{\text{ext}}$$
$$\vec{B} = \vec{\nabla} \times \vec{A} = \vec{\nabla} \times \vec{a} + \vec{B}_{\text{ext}} \tag{24}$$
$$\nabla^2 \vec{A} = \nabla^2 \vec{a} + \nabla^2 \vec{A}_{\text{ext}} = \nabla^2 \vec{a}$$

since $\nabla^2 \vec{A}_{\text{ext}} = 0$, except at the region where the external currents are non-zero. Therefore we have to solve the equation

$$\nabla^2 \vec{a} = -\frac{4\pi}{c} \vec{J}. \tag{25}$$

Due to the quantization condition the total flux is given by

$$\Phi = \Phi_a + \Phi_{\text{ext}} = n\Phi_0. \tag{26}$$

Therefore we will be considering situations where the supercurrents will generate internal magnetic fluxes such that

$$\Phi_a = (n - n_{\text{ext}})\Phi_0 \tag{27}$$

where $\Phi_{\text{ext}} = n_{\text{ext}}\Phi_0$ (we take $n_{\text{ext}}$ as a real parameter).

Let us then start from the equation

$$\frac{1}{\rho}\frac{\partial}{\partial\rho}\left(\rho\frac{\partial a_\varphi}{\partial\rho}\right) - \frac{a_\varphi}{\rho^2} = -\frac{4\pi}{c}J_\varphi. \tag{28}$$

Defining $a_\varphi = F(\rho)/\rho$, Poisson's equation reduces to

$$\frac{\partial^2 F}{\partial\rho^2} - \frac{1}{\rho}\frac{\partial F}{\partial\rho} = -\frac{4\pi}{c}J_\varphi\rho. \tag{29}$$

Since the current is given by

$$J_\varphi(\rho) = \frac{2e\hbar}{m}\sum_{i,\mu>0} f(E_i)|u_i(\mathbf{r})|^2\left[\frac{\mu - 1/2}{\rho} - \frac{e}{\hbar c}A_\varphi(\rho, z)\right]$$
$$+ [1 - f(E_i)]|v_i(\mathbf{r})|^2\left[-\frac{\mu - 1/2 + n}{\rho} - \frac{e}{\hbar c}A_\varphi(\rho)\right] \tag{30}$$

we can make the decomposition

$$-\frac{4\pi}{c}J_\varphi\rho = K(\rho) + \beta(\rho)F(\rho) \tag{31}$$

with

$$K(\rho) = \frac{8\pi|e|\hbar}{mc}\sum_i f(E_i)|u_i|^2(\mu - 1/2) + [1 - f(E_i)]|v_i|^2(\mu - 1/2 + n)$$
$$+ \frac{8\pi e^2}{mc^2}\rho A_\varphi^{\text{ext}}(\rho)\sum_i\left\{f(E_i)|u_i|^2 + [1 - f(E_i)]|v_i|^2\right\} \tag{32}$$

and

$$\beta(\rho) = \frac{8\pi e^2}{mc^2}\sum_i f(E_i)|u_i|^2 + [1 - f(E_i)]|v_i|^2. \tag{33}$$

Therefore we get

$$\frac{\partial^2 F}{\partial \rho^2} - \frac{1}{\rho}\frac{\partial F}{\partial \rho} = K(\rho) + \beta(\rho)F(\rho). \tag{34}$$

Discretizing this equation,

$$\frac{\partial^2 F}{\partial \rho^2} \rightarrow \frac{F_{i+1} - 2F_i + F_{i-1}}{a^2}$$

$$\frac{\partial F}{\partial \rho} \rightarrow \frac{F_{i+1} - F_{i-1}}{2a}$$

where $a = R/(Nr + 1)$, and $N_r + 1$ is the number of points. We get

$$\frac{F_{i+1} - 2F_i + F_{i-1}}{a^2} - \frac{F_{i+1} - F_{i-1}}{2\rho a} = K_i + \beta_i F_i. \tag{35}$$

The boundary conditions are such that $F(0) = 0$ ($a_\varphi$ does not diverge at the origin) and $\frac{\partial F}{\partial \rho}|_{\rho=R} = 0$ (**B** = 0 outside). In the first case it is enough to take $F_0 = 0$. In the second case we have $F_{N+1} - F_N = 0$. In the outside boundary, $i = N_r$, we have

$$\frac{-F_N + F_{N-1}}{a^2} - \frac{F_N - F_{N-1}}{2a(R - a)} = K_N + \beta_N F_N. \tag{36}$$

The system is therefore reduced to a tridiagonal system of equations.

The equations are solved self-consistently by choosing appropriately the first iteration. The solution converges after a few iterations (usually less than 10).

## 3. Results

The solution of the BdG equations gives full information about the superconductor within BCS theory. The equations are solved in atomic units, where $m = \hbar = e = 1$, $c = \frac{1}{\alpha} \approx 137$. We consider two sets of parameters. One set (designated set A) corresponds to an extreme case in the quantum limit and another set (designated set B) corresponds approximately to the parameters suitable for the traditional superconductor NbSe$_2$. In the first case we consider parameters such that $g = 0.8$, $E_F = 0.5$, $\omega_D = 0.25$, $R = 400$, $N_r = 1001$, $n_j = 250$ and $n_\mu = 800$, where $n_j$ is the number of zeros and $n_\mu$ is the number of angular momenta. According to these parameters we have that $\zeta_0 = v_F/\pi \Delta_0 \sim 2.45$, $k_F\zeta_0 \sim 2.45$. The critical temperature is of the order of 0.1 (all of these numbers are in atomic units). The second set of parameters is given by $g = 0.31$, $E_F = 37.2$ meV, $\omega_D = 3$ meV, $R = 12\,500$, $N_r = 1001$, $n_j = 300$ and $n_\mu = 900$. According to these parameters we have that $\zeta_0 = v_F/\pi \Delta_0 \sim 279$, $k_F\zeta_0 \sim 20.7$. The critical temperature is of the order of 8 K. (Recall that one atomic unit of distance is $\sim$0.5 Å, and that one atomic unit of energy is $\sim$27 eV.) In spite of the large difference between the two sets of parameters we will see that many of the results are similar. In the first case we consider temperatures that are rather small, of the order of $T/T_c \sim 0.001$, which corresponds to the quantum limit regime (in the case of NbSe$_2$ this regime sets in at a temperature of the order of 50 mK). The scale of the energies is such that in the first set $\Delta_0 \sim 3.53$ eV while in the second set it is of the order of $\Delta_0 \sim 1.2$ meV.

### 3.1. $\mathbf{A}^{ext}(\mathbf{r}) = 0$

We begin by reviewing the case where there is no external potential $U(\mathbf{r})$ and no explicit $\mathbf{A}^{ext}(\mathbf{r})$, in addition to a vortex line characterized by the vorticity $n$. In the first iteration we choose $\Delta(\mathbf{r}) = \Delta_0 \tanh \frac{\rho}{\zeta}$ and $\mathbf{A}(\mathbf{r}) = \mathbf{A}^{ext}(\mathbf{r}) = 0$. This is the usual way to study the

presence of a vortex line induced in the superconductor by the action of an external field, probably uniform. The energy spectra for different vorticities show the characteristic energy gap considering s-wave symmetry. For each angular momentum value there is a set of energy eigenvalues (in number given by the basis set of Bessel function zeros) with positive and negative values. The negative values give information about the positive energy values for the negative angular momenta, as explained above. The $n = 0$ solution corresponds to the absence of a vortex and is therefore the result expected in the bulk of the superconductor away from the vicinity of any vortex. For $n \geqslant 1$ the solution corresponds to a vortex with increasing vorticity. In these cases a set of bound states appears in addition to the continuum. The number of states for each angular momentum value is given by the vorticity. For $n = 1$ the boundstates are all positive (the Caroli, de Gennes and Matricon states [1]), but for $n = 2$ and $n = 3$ some of the boundstates have negative energies.

The range over which the gap function reaches its bulk value defines the coherence length. The oscillations in the various curves are eliminated if the temperature is increased, and in general the coherence length increases with the temperature (Kramer–Pesch effect). Also the coherence length increases with the vorticity.

The magnetic field is shielded in the superconductor. In the case of an $n = 1$ vortex the magnetic field decreases monotonically, evolving in the bulk to an exponential decay, which defines the penetration length, $\lambda$. As the vorticity increases, the magnetic field profile is no longer monotonic, but there is a maximum at a finite distance from the vortex. Also the penetration length increases with the vorticity, as does the coherence length. In figure 1 we compare the normalized gap functions and the normalized magnetic field for the two sets of parameters considered. In the first case we estimate a coherence length of the order of $\zeta \sim 2$ and in the second case $\zeta \sim 100$. From the decay of the magnetic field we estimate that in the first case $\lambda \sim 74$ while in the second case $\lambda \sim 1600$. This implies ratios of the order of $\lambda/\zeta \sim 37$ and $\lambda/\zeta \sim 16$, respectively.

In order for the magnetic field to be shielded an internal field is generated in the superconductor to compensate the external field. This field is generated by supercurrents that appear in the superconductor due to the motion of the Cooper pairs. At the origin there is no current since the total field equals the field entering the material through the vortex and no shielding takes place. Considering first the $n = 1$ case the current increases to compensate the external field and then decreases exponentially. The cases of higher vorticity are more complex [4]. The current is negative near the origin, then becomes positive and follows the same trend as for the singly quantized vortex. The increased winding of the phase around the vortex induces in the immediate vicinity of the vortex core currents that have opposite circulation. In figure 2 we show, for completeness, the magnetic field and the flux for the cases of $n = 1$ and $n = 2$ for NbSe$_2$ (parameters $B$).

### 3.2. External field line: solenoid of negligible width

Consider now that in addition to or instead of the uniform external field we insert in the superconductor a solenoid of negligible width. A current may be applied and the solenoid (assumed infinitely long) creates a magnetic field line of negligible width inside it and a zero field outside. The solution of the BdG equations depends both on the vorticity of the gap function and on the total field through the vector potential $\vec{A} = \vec{a} + \vec{A}_{\text{ext}}$. The external vector potential due to the thin solenoid is given in this limiting case by

$$A_{\text{ext}}^{\varphi} = \frac{n_{\text{ext}} \Phi_0}{2\pi\rho}. \tag{37}$$
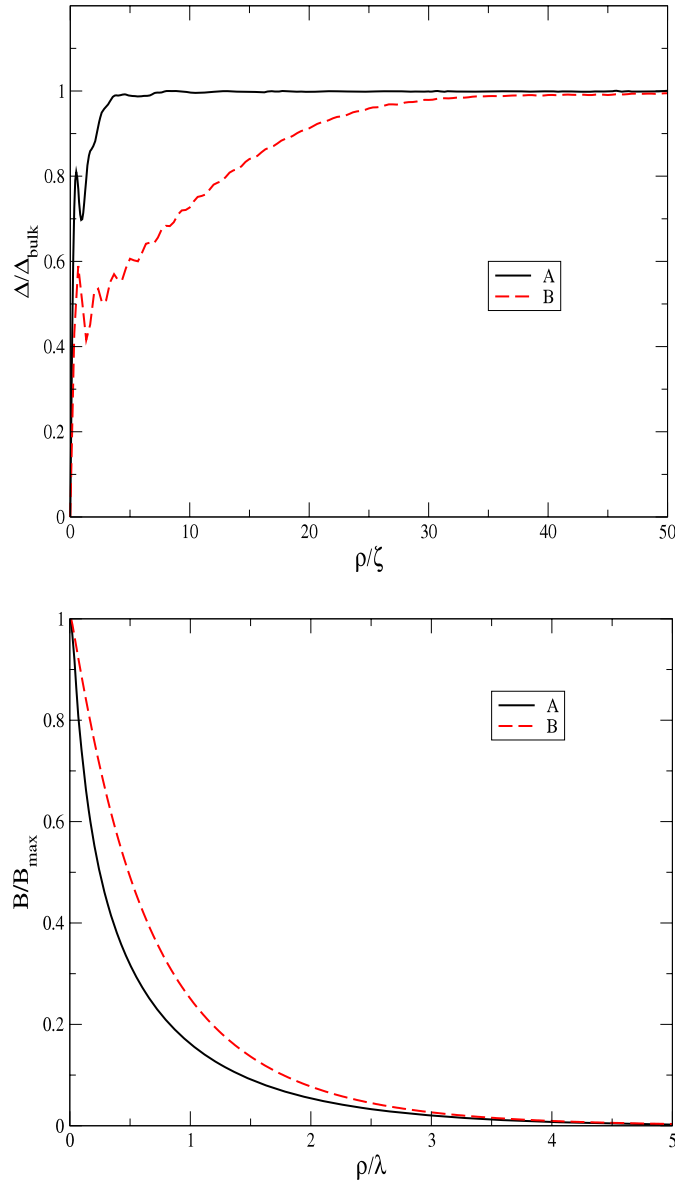
**Figure 1.** Comparison of the gap function and the magnetic field for the two sets of parameters A and B, defined in the text, at a very low temperature. We take $n = 1$ and no external solenoid ($n_{ext} = 0$). The vertical axis is scaled to the bulk value of the gap function and the value of the field at the origin, respectively, and the horizontal axis is scaled to the coherence length and the penetration length, respectively, of each set of parameters.

However, in the numerical solution we replace $\rho \rightarrow \tilde{\rho}$, where $\tilde{\rho} = \sqrt{\rho^2 + \delta^2}$ is introduced to regularize the vector potential at the origin ($\delta$ is infinitesimal). In most cases the term which includes the vector potential may be neglected in the BdG equations because it is either negligible or very small, and the main influence of the vector potential is in the expression for the current. If there is no external vector potential the internal vector potential (and consequently the total vector potential) vanishes at the axis ($a \sim \rho$). However, if the external
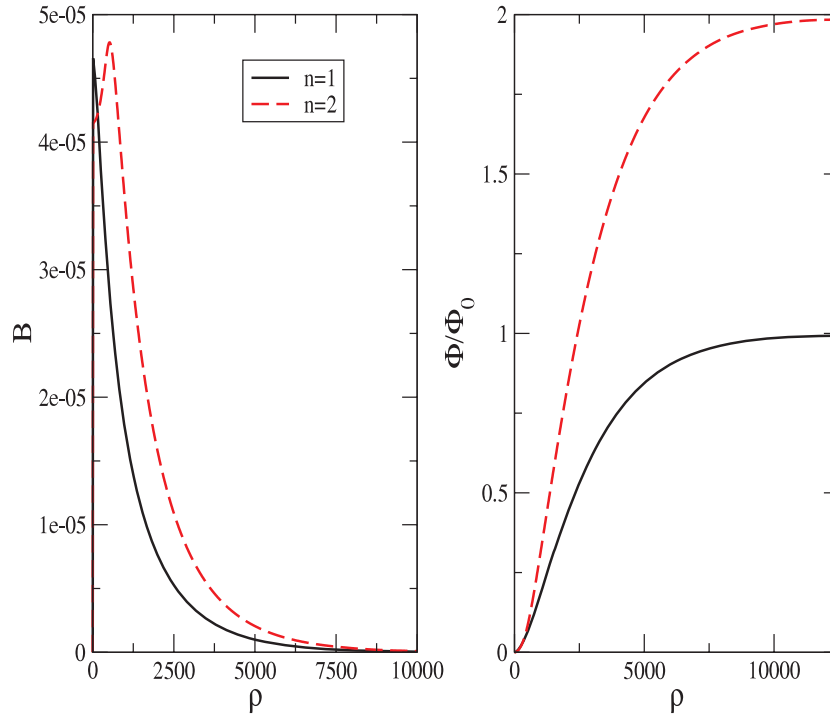
**Figure 2.** Magnetic flux and magnetic field for $n = 1$ and $n = 2$ in NbSe$_2$ (set B), with $T = 1$ K and no external solenoid.

potential has a singular form this term is important and must be taken into account. We note that we include the vector potential term in the BdG equations even though its contribution is small [2].

When the external solenoid is inserted and a field generated, one expects the right solution to be the one corresponding to a vorticity matching the total field. One may however look for other solutions of the BdG equations which eventually will have higher free energies as compared to the right solution. We will in the following consider different possible solutions of the BdG equations.

Consider again the BdG equations. Assuming that $\mathbf{A}(\mathbf{r}) = A_\varphi(\rho)\hat{e}_\varphi$ with

$$A_\varphi = n_{\text{ext}}\frac{\hbar c}{2|e|\rho} + a_\varphi \tag{38}$$

and making the general assumption of azimuthal symmetry, we can write the eigenvectors as

$$u_i = g_{\mu' j}(\rho)e^{i(\mu' - n/2)\varphi} \tag{39}$$

$$v_i = h_{\mu' j}(\rho)e^{i(\mu' + n/2)\varphi}. \tag{40}$$

Then we have

$$
\begin{aligned}
H_e u_i = \Bigg( & -\frac{\hbar^2}{2m}\left(\frac{1}{\rho}\frac{\mathrm{d}}{\mathrm{d}\rho}\left(\rho\frac{\mathrm{d}g_{\mu' j}}{\mathrm{d}\rho}\right) - \frac{(\mu' - n/2)^2}{\rho^2}g_{\mu' j} - \frac{2(\mu' - n/2)|e|}{\hbar c}\frac{a_\varphi}{\rho}g_{\mu' j} \right. \\
& \left. - \frac{(\mu' - n/2)n_{\text{ext}}}{\rho^2}g_{\mu' j} - \frac{n_{\text{ext}}^2}{4\rho^2}g_{\mu' j} - \frac{n_{\text{ext}}|e|}{\hbar c}\frac{a_\varphi}{\rho}g_{\mu' j} - \frac{e^2}{\hbar^2 c^2}a_\varphi^2 g_{\mu' j}\right) \\
& - E_{\text{F}}g_{\mu' j}\Bigg)e^{i(\mu' - n/2)\varphi}.
\end{aligned}
\tag{41}
$$

Now, grouping and simplifying the terms, the expression simplifies to

$$H_e u_i = \left( -\frac{\hbar^2}{2m} \left( \frac{1}{\rho} \frac{\mathrm{d}}{\mathrm{d}\rho} \left( \rho \frac{\mathrm{d}g_{\mu' j}}{\mathrm{d}\rho} \right) - \frac{(\mu' - n_a/2)^2}{\rho^2} g_{\mu' j} - (2\mu' - n_a) \frac{|e|}{\hbar c} \frac{a_\varphi}{\rho} g_{\mu' j} \right. \right.$$
$$\left. \left. - \frac{e^2}{\hbar^2 c^2} a_\varphi^2 g_{\mu' j} \right) - E_\mathrm{F} g_{\mu' j} \right) \mathrm{e}^{\mathrm{i}(\mu' - n/2)\varphi} \tag{42}$$

where $n_a = n - n_\mathrm{ext}$. For $H_e^* v_i$, the expression can be obtained from this one, by replacing $u_i$ by $v_i$ and $\mathbf{A}$ by $-\mathbf{A}$. The first replacement is equivalent to making

$$g_{\mu' j} \to h_{\mu' j}, \qquad n \to -n \tag{43}$$

and the second is equivalent to

$$n_\mathrm{ext} \to -n_\mathrm{ext}, \qquad a_\varphi \to -a_\varphi. \tag{44}$$

So, $H_e^* v$ is given by

$$H_e^* v_i = \left( -\frac{\hbar^2}{2m} \left( \frac{1}{\rho} \frac{\mathrm{d}}{\mathrm{d}\rho} \left( \rho \frac{\mathrm{d}h_{\mu' j}}{\mathrm{d}\rho} \right) - \frac{(\mu' + n_a/2)^2}{\rho^2} h_{\mu' j} + (2\mu' + n_a) \frac{|e|}{\hbar c} \frac{a_\varphi}{\rho} h_{\mu' j} \right. \right.$$
$$\left. \left. - \frac{e^2}{\hbar^2 c^2} a_\varphi^2 h_{\mu' j} \right) - E_\mathrm{F} h_{\mu' j} \right) \mathrm{e}^{\mathrm{i}(\mu' + n/2)\varphi}. \tag{45}$$

So the explicit dependence on $n$ and $n_\mathrm{ext}$ comes only through $n_a$.

The same choices for the vector potential and for the eigenfunctions lead to the current in the form

$$J_\varphi = -\frac{2|e|\hbar}{m} \sum_{\mu' j} f(E_{\mu' j}) g_{\mu' j}^2 \left( \frac{\mu' - n_a/2}{\rho} + \frac{|e|}{\hbar c} a_\varphi \right)$$
$$+ \left( 1 - f(E_{\mu' j}) \right) h_{\mu' j}^2 \left( \frac{-\mu' - n_a/2}{\rho} + \frac{|e|}{\hbar c} a_\varphi \right). \tag{46}$$

Also, the Maxwell equation becomes

$$\frac{1}{\rho} \frac{\partial}{\partial \rho} \left( \rho \frac{a_\varphi}{\partial \rho} \right) - \frac{a_\varphi}{\rho^2} = \frac{8\pi |e|\hbar}{mc} \sum_i f(E_{\mu j}) g_{\mu j}^2 \left( \frac{\mu - n_a/2}{\rho} + \frac{|e|}{\hbar c} a_\varphi \right)$$
$$+ \left( 1 - f(E_{\mu j}) \right) h_{\mu j}^2 \left( \frac{-\mu - n_a/2}{\rho} + \frac{|e|}{\hbar c} a_\varphi \right). \tag{47}$$

So neither the BdG equations, nor the Maxwell equation, depends on $n$ or $n_\mathrm{ext}$, separately, but rather on the difference $n_a = n - n_\mathrm{ext}$. The solution of the spectrum, eigenfunctions and all quantities derived from these are only a function of $n_a$. The singular term of the external field line has the effect of renormalizing the states of the Bessel function basis if the external flux is a multiple of the quantum of flux. In particular, when $n - n_\mathrm{ext} = n_a = 0$ the system has an effective zero vorticity. However, the total flux is determined by $n$, as we will see.

If we consider the combined transformations $n_a \to -n_a$, $a_\varphi \to -a_\varphi$ and $\mu' \to -\mu'$ the equations are invariant. This is equivalent, as we saw before, to making the combined transformations $n_a \to -n_a$, $a_\varphi \to -a_\varphi$, and $E_i \to -E_i$, $g \to h$ and $h \to -g$. Under these transformations the gap function remains invariant and the current changes sign, as expected.

In figure 3 we plot the flux as a function of distance for two different vorticities $n = 0$ and $n = 1$ for different applied fields. The total field is determined by the choice of vorticity of the solution: in the case of $n = 0$ the total flux in the bulk vanishes and in the case of $n = 1$ the total flux in the bulk equals a quantum of flux. The external field is determined by the current that goes through the infinitely thin solenoid. This is parameterized by the flux $\Phi_\mathrm{ext} = 0.5, 1, 1.5, 2\Phi_0$. The fully self-consistent solution of the BdG equations yields the
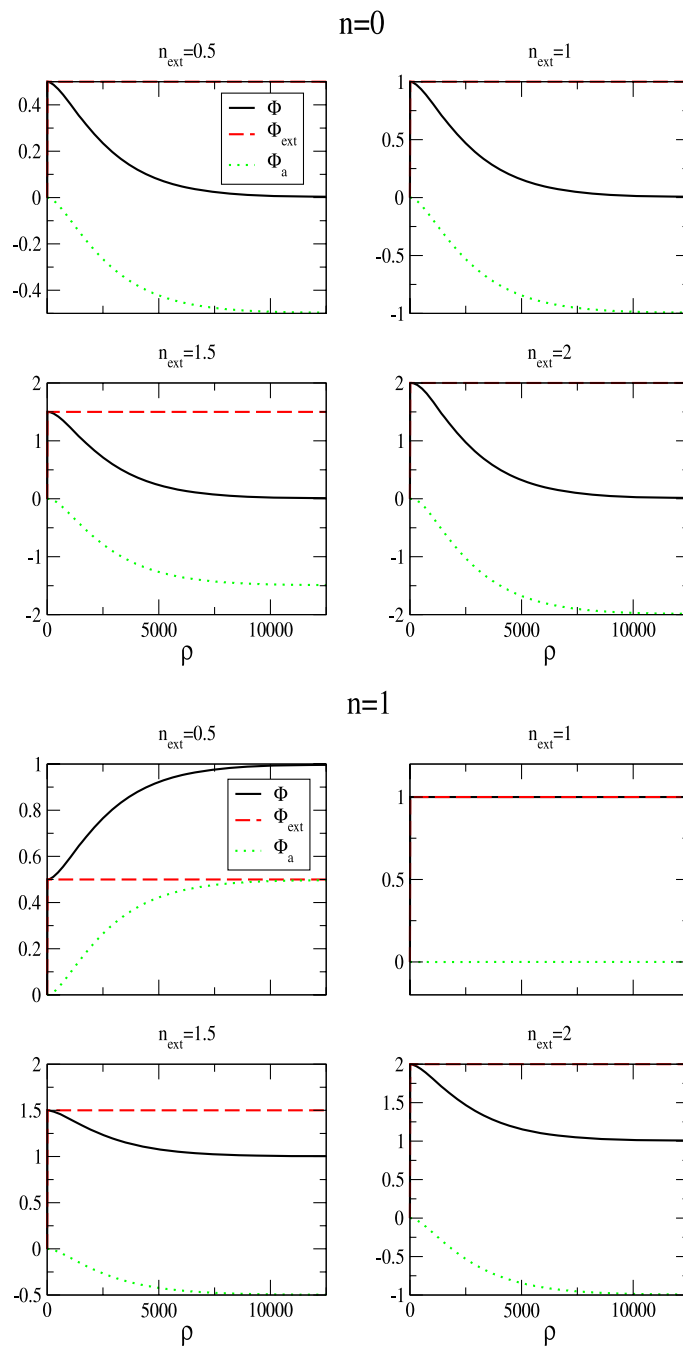
**Figure 3.** Magnetic flux (internal, external and total), for $n = 0$ (top panel) and for $n = 1$ (bottom panel) and different $n_{ext}$ in NbSe$_2$ (set B), with $T = 1$ K.

internal vector potential $\vec{a}$ generated by the supercurrents carried by the quasiparticles. The flux originated by the internal field compensates the external flux in order to give the correct total flux fixed by the chosen vorticity, $n$. As we can see in figure 3, for all values of the external

field, the internal field is negative in order to compensate and give a zero total flux in the bulk. In the case of $n = 1$ the value of $\Phi_{\text{ext}} = 0.5\Phi_0$ is smaller than the total flux and the internal vector potential is positive. For $\Phi_{\text{ext}} = \Phi_0$ the internal field is zero and for the higher values of $\Phi_{\text{ext}}$ the internal field is again negative, as explained above.

In figure 4 we show the energy spectra corresponding to the cases discussed in figure 3 and compare with the case with no external line ($n_{\text{ext}} = 0$). When the external field is higher than the total field and, therefore, the internal field is negative, there appear boundstates of negative energy in number $n_{\text{ext}} - n$. When the external field is smaller, positive energy boundstates appear in number $n - n_{\text{ext}}$. When the two numbers match there are no bound states, corresponding to a zero internal field. The boundstates are therefore associated to a non-vanishing internal field. Positive energies correspond to a positive internal field and negative energies to a negative internal field. When $n_{\text{ext}}$ is an integer the external field can be absorbed in the basis functions and there is no remaining field affecting the BdG equations (except for the internal field, which gives a small contribution). This is determined by $n_a$. If $n_a = 0$ there is no field left (external or internal) and this is equivalent to a system with no vortex. In this case there are no boundstates, the gap function is uniform and there are no supercurrents.

In figure 5 we show the influence of the external field line on the gap function. The results are presented for the case of NbSe$_2$. When the solenoid external field is superimposed, the shape is altered. As mentioned above, the shape of the gap function depends essentially on the difference $n_a = n - n_{\text{ext}}$. We compare different values of $n_a$. As $n_a$ increases the coherence length increases. In the limit when $n_a = 0$ the gap function is constant.

A consistent explanation can be obtained by looking at the magnetic field and supercurrent profiles. In figure 6(a) we compare the magnetic field profiles and in figure 6(b) we compare the supercurrent profiles. In this last case we also consider the case of $n = 2$. As stated above, when the external field is larger than the total field, fixed by the vorticity of the solution, the magnetic field is negative near the vortex and tends to zero exponentially from negative values. When the external field $n_{\text{ext}} = n$ the field is zero and when $n_{\text{ext}} < n$ the field is positive as in the case of the vortex line. This is clearly shown in figure 6. The behaviour of the induced supercurrents is more complex. It is also a function of $n - n_{\text{ext}}$. When this difference is zero the current is zero. When $n - n_{\text{ext}} > 0$ we have a behaviour similar to the one for the vortex line with no external field: when $n - n_{\text{ext}} = 1$ the current is positive, going through a maximum and then decreasing, and for larger values of $n - n_{\text{ext}}$ the current has a node.

### 3.3. External solenoid of finite width

Consider now a long solenoid of finite width. As mentioned above, it could also be a long magnetic whisker inserted in the material or a magnetic dot with an extra homogeneous field parallel to the magnetic moment of the dot, taken as perpendicular to the superconductor plane. The width of the solenoid is given by $R_s$. We consider two cases: $R_s = 1$ and $R_s = 50$. The first case is very similar to the thin solenoid since the coherence length is of the same order. However, the thicker solenoid has a width that is considerably larger than the coherence length and is of the same order as the penetration length. The external vector potential is now given by

$$A_{\text{ext}}^{\varphi} = \theta(R_s - \rho)\frac{n_{\text{ext}}\Phi_0}{2\pi R_s^2}\rho + \theta(\rho - R_s)\frac{n_{\text{ext}}\Phi_0}{2\pi\rho}. \tag{48}$$

Also, we consider two cases. The first case is achieved by considering an external potential $U(\vec{r})$ that is strongly repulsive in the region occupied by the solenoid. This effectively restricts the presence of the superconducting pairs in the solenoid. A value of $U(\mathbf{r}) = U\Theta(R_s - \rho)$, with $U = 50$, is quite efficient and is such that the material inserted in the superconductor is
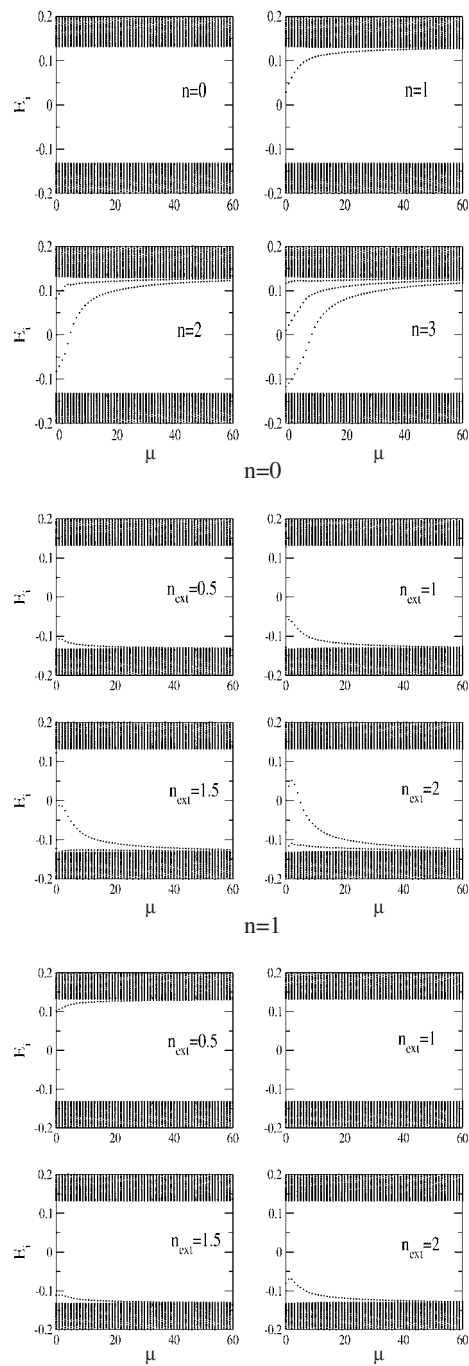
**Figure 4.** Energy spectra for (set A) (top) different vorticities $n = 0, n = 1, n = 2, n = 3$, with $n_{\text{ext}} = 0$; (middle) $n = 0$ for various external fields 0.5, 1.1.5, 2. Note the appearance of negative energy boundstates as the field increases; (bottom) $n = 1$ for various external fields 0.5, 1.1.5, 2. Note the appearance of a positive energy boundstate at a field smaller than the vorticity and negative energy boundstates as the field increases. Also note the absence of boundstates for a field 1.
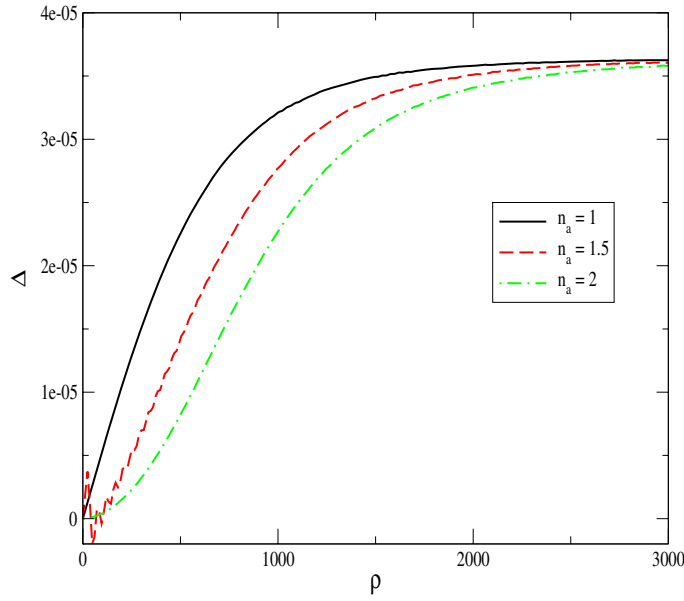
**Figure 5.** Gap function for NbSe$_2$ (set B) for different values of $n_a = n - n_{\text{ext}}$.

opaque and the electrons cannot penetrate. This can be achieved by either inserting a solenoid in a hole punched into the superconductor, or inserting a magnetic rod with a thin insulating layer wrapped around it. One could also consider the solution of the BdG equations imposing a boundary condition such that the electrons do not penetrate the inner region. It is however much easier and similar to impose a strong repulsive potential. We should stress however that the two procedures are not strictly the same. As we will see later, the strongly repulsive potential imposes that the gap function vanishes at the interface (or is very small) since the electrons cannot penetrate the interface and, therefore, there are no paired electrons. In the traditional approach the gap function is finite at the interface as obtained in the context of the Ginzburg–Landau framework [7]. We stress however that this approach is only valid for scales larger than $\xi_0$.

The effect of the repulsive potential leads in the BdG equations to the simplified expressions

$$
\begin{aligned}
I_3^- &= U W^- \\
I_3^+ &= U W^+
\end{aligned}
\tag{49}
$$

where

$$
W^- = \int_0^{R_s} \phi_{j,\mu-1/2}(\rho)\phi_{j',\mu-1/2}(\rho)\rho \, \mathrm{d}\rho
\tag{50}
$$

$$
W^+ = \int_0^{R_s} \phi_{j,\mu-1/2+n}(\rho)\phi_{j',\mu-1/2+n}(\rho)\rho \, \mathrm{d}\rho.
\tag{51}
$$

In the other case we take $U = 0$, and therefore the electrons are allowed to penetrate the finite width region where a magnetic field is inserted in the superconductor. This case is probably harder to test experimentally since it would imply a solenoid inserted in the body of the superconductor, consisting of a very thin wire such that the electrons might penetrate its interior with negligible scattering. It is a somewhat idealized situation but allows us to isolate
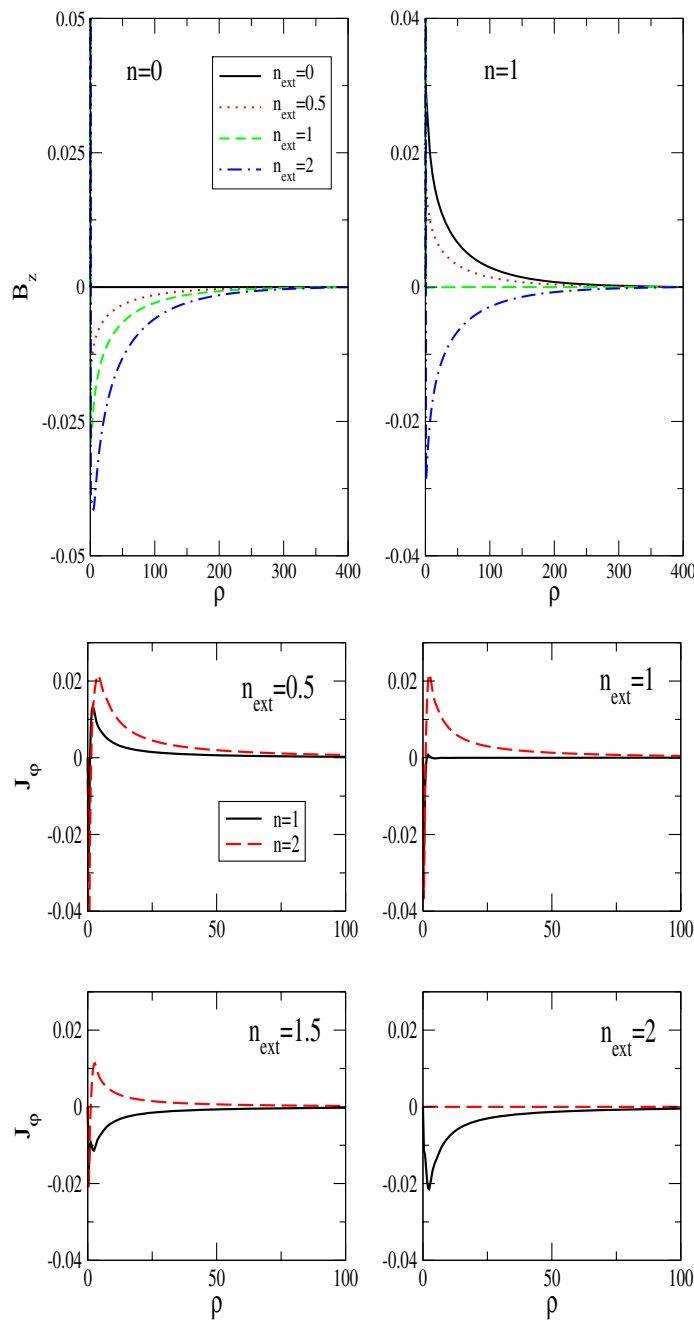
**Figure 6.** (a) Magnetic field profiles for the various external field values for $n = 0, n = 1$ and for set A. Note the opposing magnetic fields when $n_{ext} > n$ changes to $n_{ext} < n$. (b) Induced supercurrents for the various external fields for the solutions with $n = 1, n = 2$ for set A. Note the changes of signal close to the vortex location.

the effect of the finite width region with magnetic field on the superconductor from the inherent space constraint due to the physical presence of the solenoid.

Consider first the energy spectra. The case of $R_s = 1$ is qualitatively similar to the vortex line and there is a set of boundstates as before characterized by $n_a$. Even though the vector potential is not singular if the width is very small there is a large component of the vector potential and the numerical solution does not distinguish this case from a truly singular potential. When the thickness is larger than the coherence length the structure of the boundstates is changed. In the case of the opaque solenoid the boundstates disappear altogether since the pair density near the origin vanishes, due to the repulsive potential. If the solenoid is transparent, the electrons can probe the solenoid core. However, since the magnetic field is spread through a finite region, the spectrum depends mainly on the vorticity and only weakly on the external flux. The effect is not strong enough to change the nature of the boundstates. In this case there is no singular term and the spectrum is not qualitatively changed. The number of boundstates is therefore characterized by the vorticity of the gap function, $n$. This is shown in figure 7, where we compare the energy spectra for the two cases of $U = 50$ and $U = 0$. The effect of the solenoid on the gap function is shown in figure 8, where the two solenoids are also compared. Note that as the opaque solenoid is approached, the gap function vanishes and displays oscillations. This is in contrast with the interface between a superconductor and the vacuum where the gap function is finite very close to the interface.

The effects of the solenoid are best seen in the magnetic field profiles. In figure 9 we compare the magnetic field for the two solenoids for different cases. When the vorticity $n < n_{ext}$ the magnetic field for $\rho > R_s$ is negative, to compensate the field introduced by the external solenoid. This does not happen when $n > n_{ext}$ since the external solenoid field does not exceed the field that would correspond to the vorticity selected. Also, note the difference at small distances between the opaque and the transparent solenoid. The field at small distances in the opaque solenoid is determined by $n_{ext}$ which creates a uniform field and determined by the supercurrents distributed for $\rho > R_s$, which create an opposing uniform field inside the solenoid. In the case of the transparent solenoid the Cooper pairs can penetrate the small distance region and feel the singular nature of the vortex line implied by the selected form of the gap function.

In figure 10 we show the flux for the opaque solenoid for $n = 1$ with and without current flowing through the solenoid, for the two different widths. When $n_{ext} = 1$ the flux saturates in the vicinity of the core for the smaller solenoid. However, in the case of the larger solenoid the flux just follows the usual classical trend due to the constant value of the magnetic field inside the solenoid, assumed of infinite length. In the vortex line the field decreases from the core while in the solenoid it is constant.

### 3.4. Magnetic rod

We consider now an infinitely long ferromagnet inserted in the superconductor. The parameters used are those corresponding to set B. The Hamiltonian is changed into the form

$$H \rightarrow H + h \int d^2r \sum_\sigma \sigma c_\sigma^\dagger c_\sigma \tag{52}$$

where $h$ is the exchange field taken as constant inside the ferromagnet. In the ferromagnet we assume that $\Delta = 0$ ($g = 0$). The BdG equations are now written in the form

$$\left[\frac{1}{2m}\left(\mathbf{p} - \frac{e}{c}\mathbf{A}\right)^2 + h - E_F\right]u_{i,\uparrow}(\mathbf{r}) + \Delta(\mathbf{r})v_{i,\downarrow}(\mathbf{r}) = E_i u_{i,\uparrow}(\mathbf{r})$$

$$-\left[\frac{1}{2m}\left(\mathbf{p} + \frac{e}{c}\mathbf{A}\right)^2 - h - E_F\right]v_{i,\downarrow}(\mathbf{r}) + \Delta^*(\mathbf{r})u_{i,\uparrow}(\mathbf{r}) = E_i v_{i,\downarrow}(\mathbf{r}) \tag{53}$$
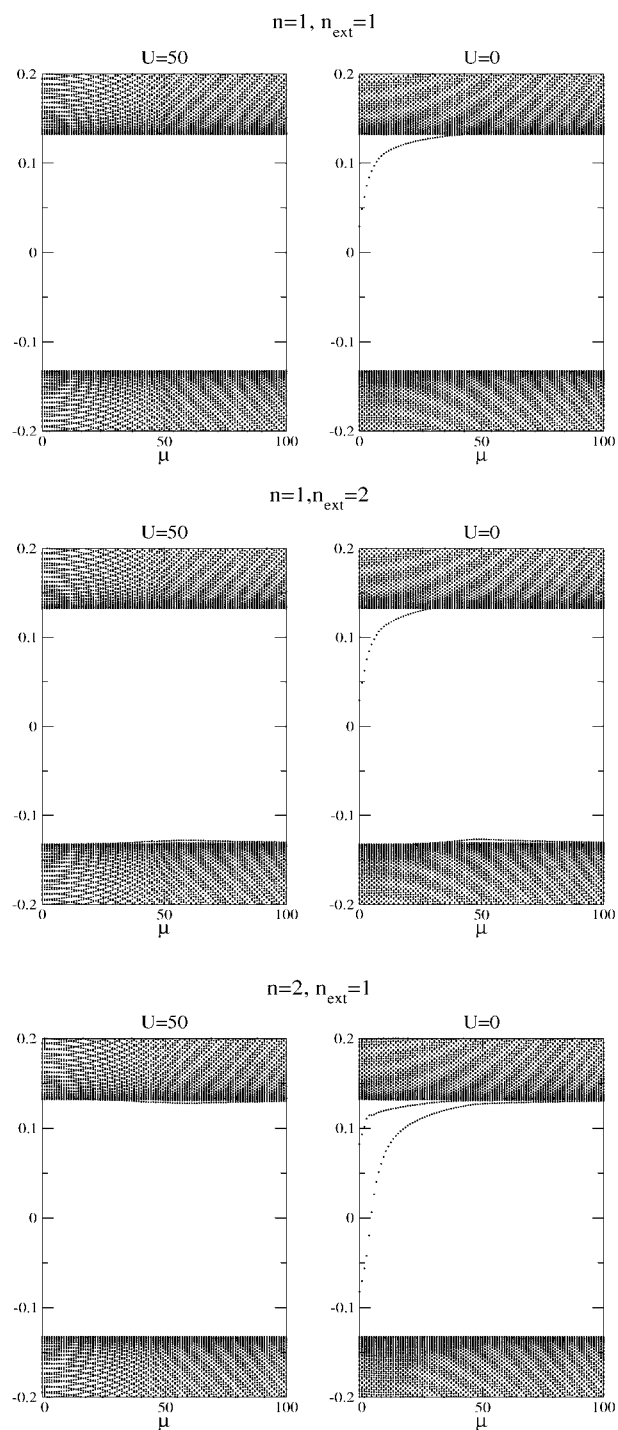
**Figure 7.** Energy spectra for two solenoids with and without repulsion for different vorticities and external fields for set A.
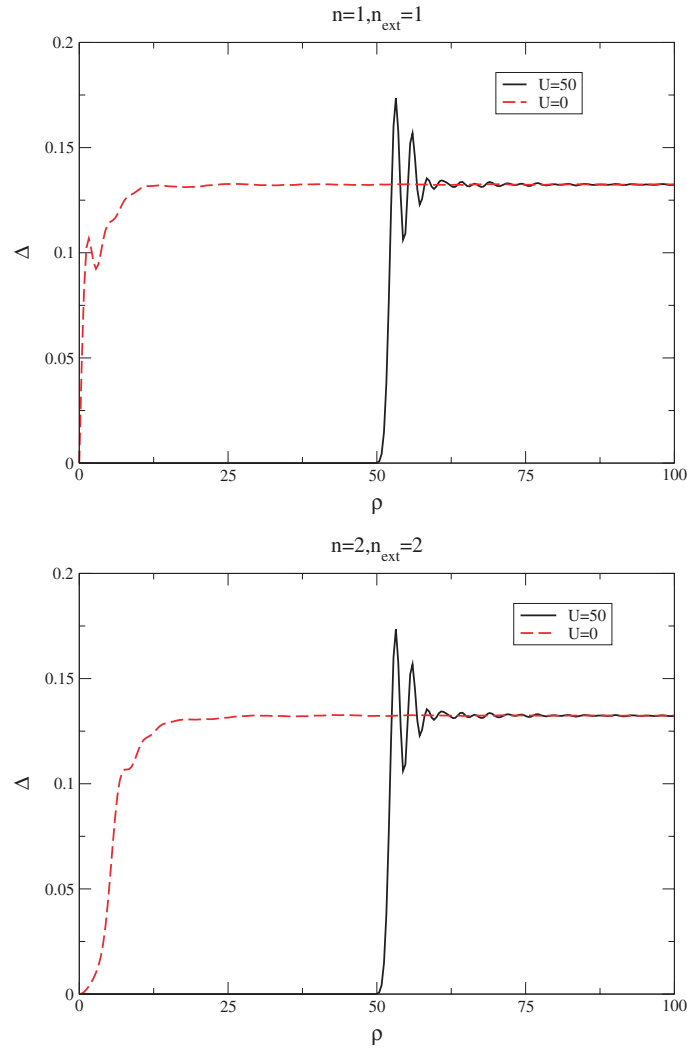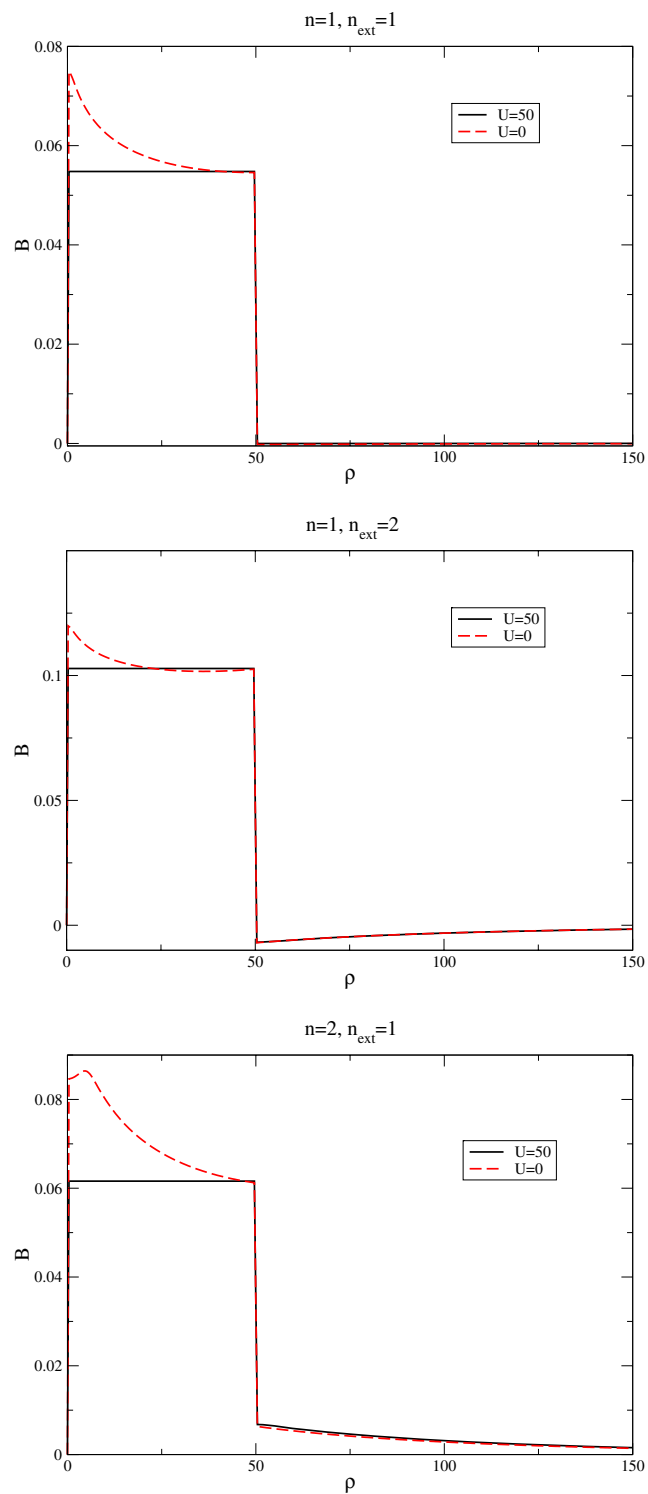
**Figure 8.** Gap function for two solenoids with and without repulsion for different vorticities and external fields for set A.

and similar equations exist for $u_{i,\downarrow}$ and $v_{i,\uparrow}$ [7]. We take $U = 0$. Since the exchange field is along the $z$-direction, there is no spin flipping and it is enough to solve the equations for one spin component. There is a symmetry involved that allows to obtain the solutions for the other component since if $(u_{\uparrow}, v_{\downarrow})$ is a solution for the eigenvalue $E$, then $(v_{\uparrow}^{*}, -u_{\downarrow}^{*})$ is a solution with eigenvalue $-E$.

In the solution of the problem using the same basis as above we replace

$$
\begin{aligned}
T^{-} &\to T^{-} + hW^{-} \\
T^{+} &\to T^{+} + hW^{+} \\
\Delta_{jj'} &= \int_{R_{s}}^{R} \phi_{j,\mu-1/2}(\rho)\Delta(\rho)\phi_{j',\mu-1/2+n}(\rho)\rho \, d\rho.
\end{aligned}
\tag{54}
$$

**Figure 9.** Magnetic field profiles for two solenoids with and without repulsion for different vorticities and external fields for set A.
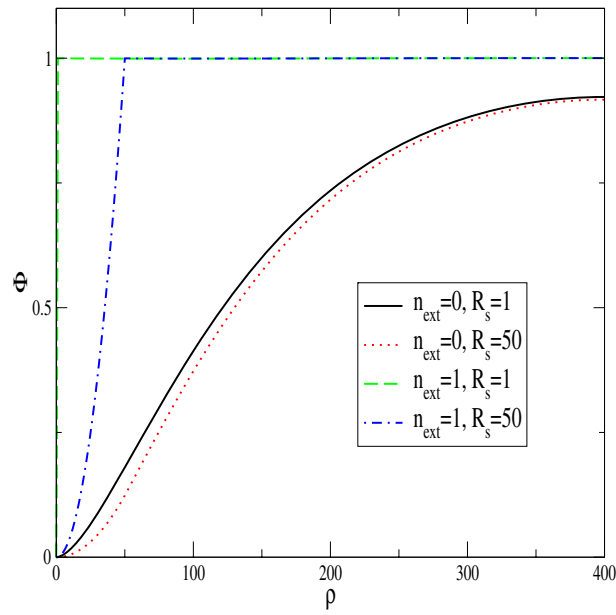
**Figure 10.** Flux as a function of distance for $n = 1$ and external fields $A_x = 0$, $A_x = 1$ for different widths of the opaque solenoid for set A.

The vector potential is given by equation (48). We relate $B_{ext}$ with $h$ like $B_{ext}/\Phi_0 = 2 \times 10^{-3}h$. We stress again that we are assuming that the external field lines do not penetrate the superconductor for $\rho > R_s$.

We consider different values of the exchange field corresponding to different numbers of flux quanta through the magnetic rod. We consider fields $h = 4 \times 10^{-5}, 4 \times 10^{-4}, 4 \times 10^{-3}$, from a small field to a rather large one. They correspond to external fluxes $\Phi \sim 0.25\Phi_0, 2.5\Phi_0, 25\Phi_0$, respectively. This is shown in figure 11, where we compare the total flux, external and internal fluxes for the various fields and different vorticities, $n$. The results follow the same trend as for the solenoid considered above outside the region of the magnet. Once again the total flux is fully determined by the vorticity of the gap function, $n$. However, inside the magnet the total flux is larger than the external field due to the positive contribution of the internal field. In the solenoid case the internal field opposes the external field and the total flux is smaller than the external flux. This is qualitatively different from the other cases we have been considering. This behaviour distinguishes the magnet from the solenoid.

In figures 12–14 we present the energy levels for the various fields and vorticities. At intermediate values of the angular momentum the number of boundstates follows the same trend as before (note that in most cases $n_a < 0$ and, therefore, the boundstates are at negative energies). At small angular momentum the structure of the states is changed due to the magnetic order in the rod.

Even though we have selected $g = 0$ inside the magnet, and therefore $\Delta$ vanishes inside it, due to the proximity effect the superconducting correlations penetrate in the magnetic rod (and vice versa). In figure 15 we show results for $\Delta(\rho)/g \sim \langle cc \rangle$ and we see that, for small and moderate exchange field, the superconducting correlations penetrate in the rod, as is well known [30].

As is well known [30], the exchange field induces a finite momentum for the Cooper pairs and produces damped space oscillations of the superconducting correlations in the magnetic
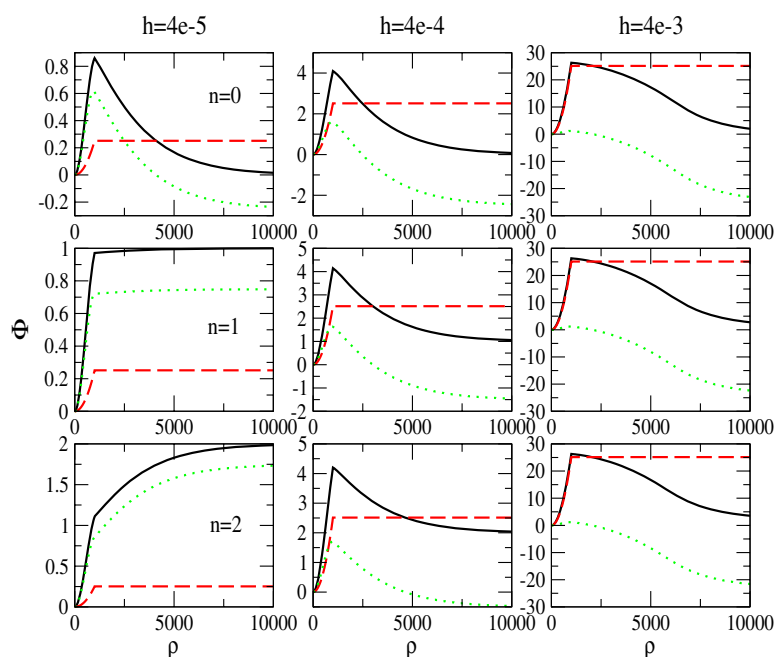
**Figure 11.** Total flux (solid lines), external flux (dashed lines) and internal flux (dotted lines) for various exchange fields and vorticities.
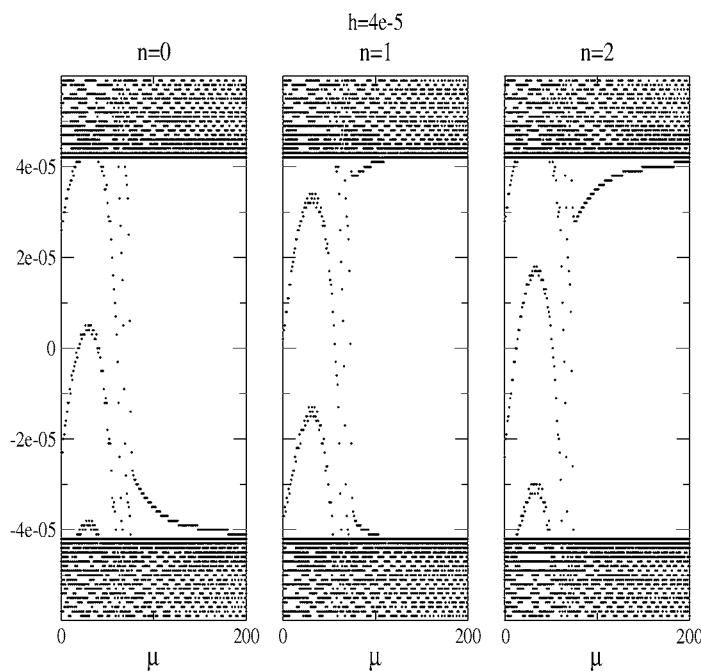


**Figure 12.** Energy levels for $h = 4 \times 10^{-5}$ and vorticities $n = 0, 1, 2$.

system. This is clearly seen in figure 16(a). Near the origin, and due to the finite size effect, the damping of the oscillations is affected for the smaller fields. If the field is of moderate size
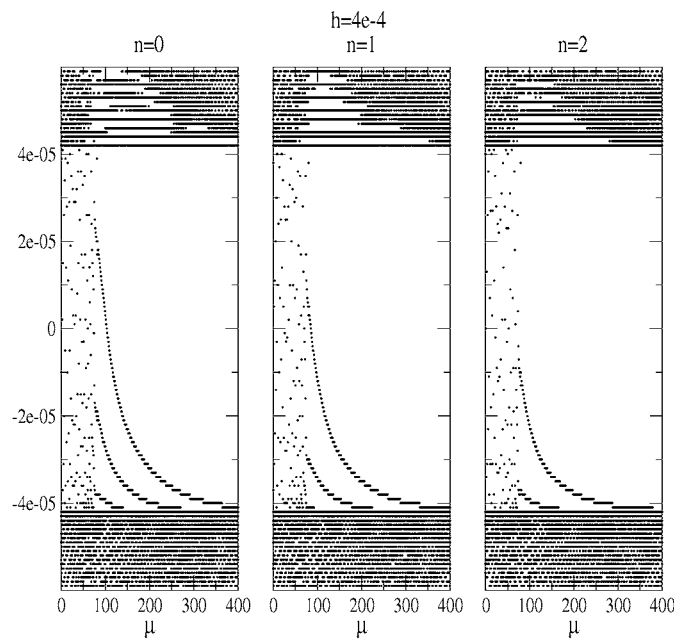
**Figure 13.** Energy levels for $h = 4 \times 10^{-4}$ and vorticities $n = 0, 1, 2$.
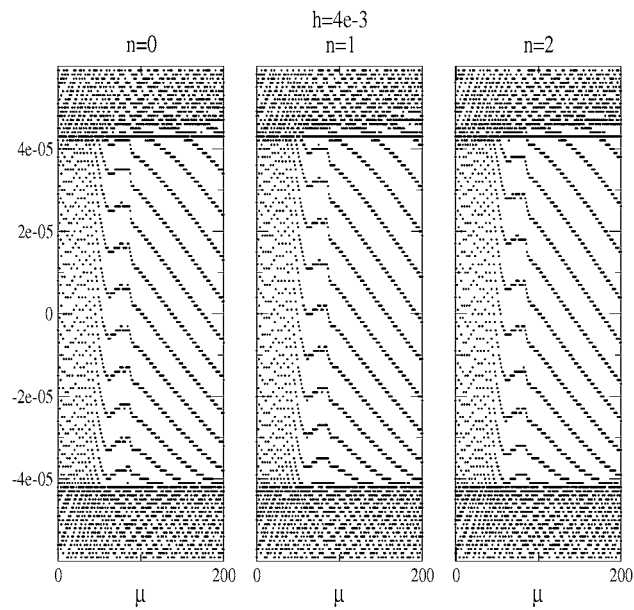


**Figure 14.** Energy levels for $h = 4 \times 10^{-3}$ and vorticities $n = 0, 1, 2$.

the oscillations are damped far from the origin, as for a semi-infinite medium. In figure 16(b), we show the effect of the finite size. Choosing an intermediate exchange field we see that on increasing the rod radius the amplitude at the origin decreases substantially. Also, from figure 16(a) we see that for the larger field we have considered, the superconducting correlations are suppressed to large distances. This is shown again in figure 17, where we consider the same
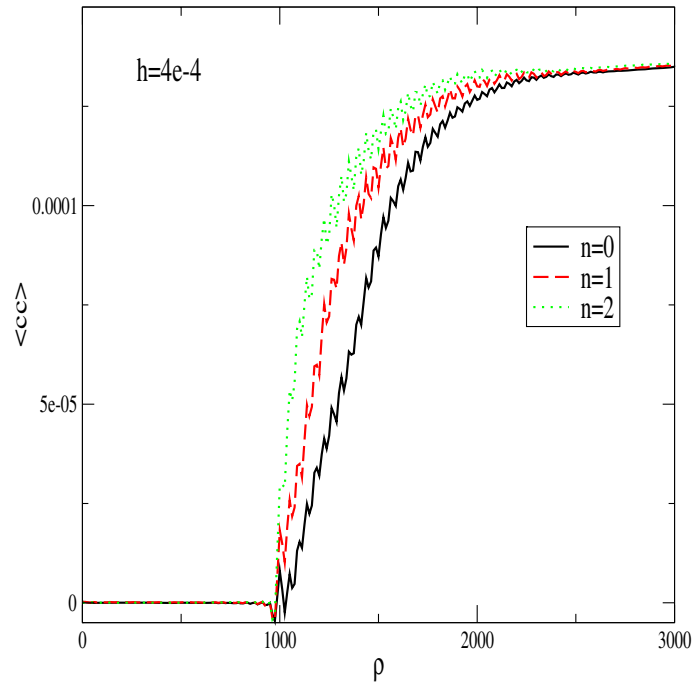
**Figure 15.** Superconducting correlations for an exchange field $h = 4 \times 10^{-4}$ corresponding approximately to a flux of $\Phi \sim 2.5\Phi_0$, for vorticities $n = 0$ ($n_a \sim -2.5$), $n = 1$ ($n_a \sim -1.5$) and $n = 2$ ($n_a \sim -0.5$).

field corresponding to a flux of the order of $\sim 25\Phi_0$ and compare the cases of a flux line, the transparent solenoid and the magnetic rod. Since the field is so large, $\Delta$ is depleted up to large distances [9]. For such a large flux $\Delta \sim 0$ up to distances that are significantly larger than the radius of either the solenoid or the magnetic rod. For this large flux there is in the case of the magnetic rod an inner core which is magnetic, then a normal region (since $\Delta$ is vanishing small) and then the superconducting bulk system.

## 4. Conclusions

In this work we have revisited the problem of a vortex in a superconductor. There are several reasons that led us to carry out this study. First of all there has been an increased interest in the interplay of magnetic and superconducting materials both from the point of view of the influence of the superconductivity on the magnetic materials but also the influence of the magnetic materials on the superconductivity. In particular, the vicinity of magnetic dots near the superconductor may serve as pinning centres and the motion of vortices in the superconductor may induce the motion of magnetic domain walls in magnetic materials. These properties may be of importance for the control of dissipation in the superconductor and the control of magnetic registers in the magnetic materials, respectively. The studies carried out before have shown the possibility of observation of giant vortices and therefore we have considered in this work different vorticities and studied the current and gap function profiles.

An interesting problem to be considered is the penetration of a magnetic rod or solenoid in the bulk of the superconductor. We have considered these situations and studied the response of the superconductor as a function of the vorticity around the external field lines. We have
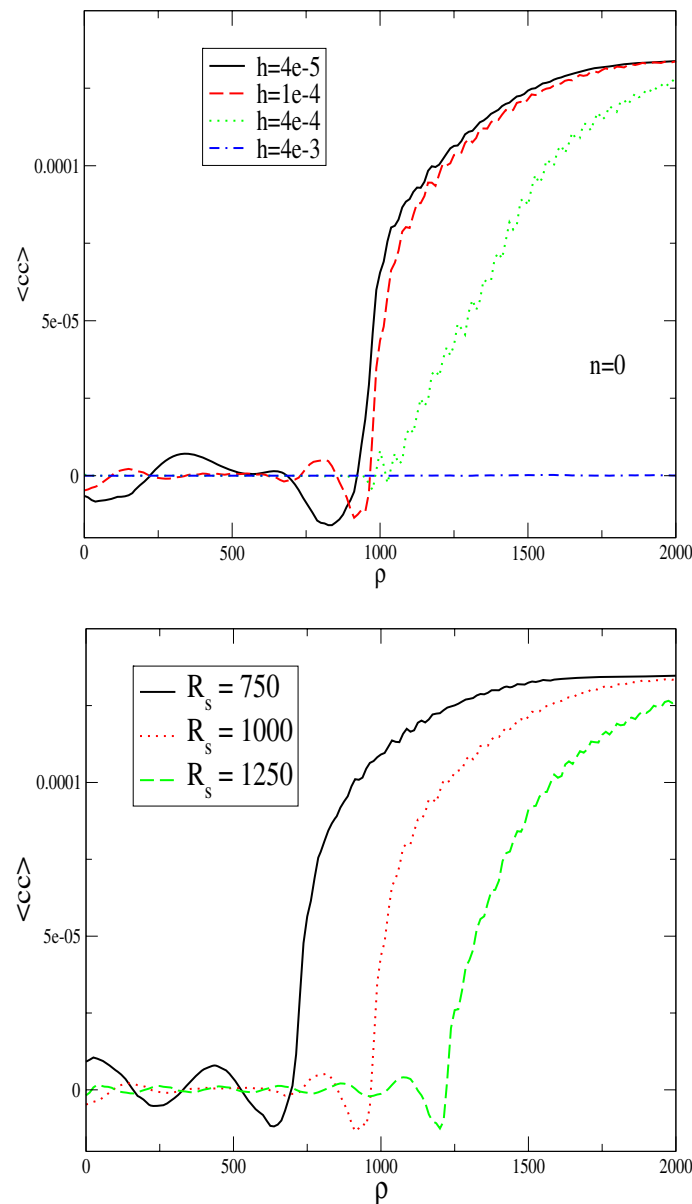
**Figure 16.** Proximity effect of the superconducting correlations inside the magnet (a) as a function of field and (b) as a function of rod radius.

confirmed by a fully self-consistent calculation that the winding of the phase of the gap function determines the properties of the system, with the notable exception of an infinitely thin solenoid. In this case there is an effective vorticity, $n_a$, which determines the nature of the spectrum. We established a detailed connection between the vorticity, the induced internal currents and the energy spectrum structure. Also, we compared the cases of the solenoid and the magnetic rod and studied the influence of the exchange field in the behavior of the magnetic properties, which reveals itself particularly at small distances from the axis.
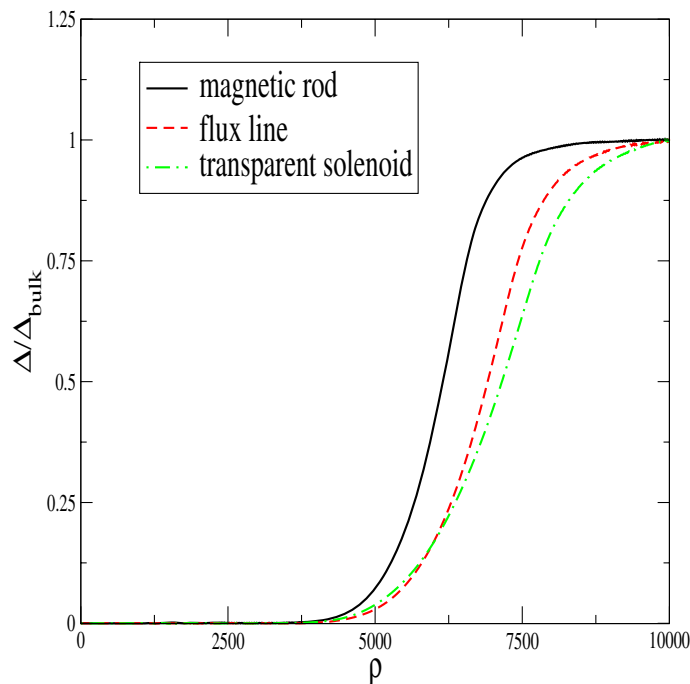
**Figure 17.** Graph of the gap function normalized to its bulk value for the large exchange field $h = 4 \times 10^{-3}$ for the cases of a vortex line, the transparent solenoid and the magnetic rod (for the set of parameters $B$).

An extension of this problem is to consider a superconductor in a finite slab and to insert two magnetic rods from opposite sides with either the same or opposite polarities. At the tip of each rod (or solenoid) the magnetic field lines will either leave or enter the superconductor. Due to the Meissner effect these field lines will be confined to flux tubes in a way similar to the confinement of the chromodynamic field. Far from the solenoid ends the system looks very much like the problem studied here: a single infinite solenoid inserted in a superconductor. The behaviour near the solenoid tips is quite interesting, for it provides an explicit realization of the confinement problem. This problem will be considered elsewhere.

## Acknowledgment

## References

[1] Caroli C, de Gennes P G and Matricon J 1964 *Phys. Lett.* **9** 307
[2] Gygi F and Schlüter M 1991 *Phys. Rev.* B **43** 7609
[3] Franz M and Tesanovic Z 1998 *Phys. Rev. Lett.* **80** 4763
[4] Rainer D, Sauls J A and Waxman D 1996 *Phys. Rev.* B **54** 10094
[5] Hayashi N, Isoshima T, Ichioka M and Machida K 1998 *Phys. Rev. Lett.* **80** 2921
[6] Kramer L and Pesch W 1974 *Z. Phys.* **269** 59
    See also Brandt E H 1976 *J. Low Temp. Phys.* **24** 409
    See also Brandt E H 1976 *J. Low Temp. Phys.* **24** 427
    Brandt E H 1976 *Phys. Status Solidi* b **77** 105

[7] de Gennes P G 1989 *Superconductivity of Metals and Alloys* (Reading, MA: Addison-Wesley)
[8] Volovik G E 1993 *JETP Lett.* **57** 244
[9] Virtanen S M M and Salomaa M M 1999 *Phys. Rev.* B **60** 14581
[10] Virtanen S M M and Salomaa M M 2000 *Physica* B **284–288** 741
[11] Hasegawa S, Matsuda T, Endo J, Osakabe N, Igarashi M, Kobayashi T, Naito M, Tonomura A and Aoki R 1991 *Phys. Rev.* B **43** 7631
[12] Nishio T, Okayasu S, Suzuki J-i and Kadowaki K 2004 *Physica* C **412–414** 379
[13] Little W and Parks R D 1962 *Phys. Rev. Lett.* **9** 9
[14] Karapetrov G, Fedor J, Iavarone M, Rosenmann D and Kwok W K 2005 *Phys. Rev. Lett.* **95** 167002
[15] Tanaka Y, Kashiwaya S and Takayanaki H 1995 *Japan. J. Appl. Phys.* **34** 4566
[16] Lyuksyutov I F and Pokrovsky V 2000 *Mod. Phys. Lett.* **14** 409
[17] Lyuksyutov I F and Pokrovsky V 2005 *Adv. Phys.* **54** 67
[18] Buzdin A I 2005 *Rev. Mod. Phys.* **77** 935
[19] Berciu M, Rappoport T G and Janko B 2005 *Nature* **435** 71
[20] Erdin S 2005 *Phys. Rev.* B **72** 014522
[21] Lyuksyutov I F and Pokrovsky V 1998 *Phys. Rev. Lett.* **81** 2344
[22] Lyuksyutov I F and Naugle D G 1999 *Mod. Phys. Lett.* **13** 491
[23] Lyuksyutov I F and Naugle D G 2000 *Physica* C **341–348** 1267
[24] Erdin S, Kayali A F, Lyuksyutov I F and Pokrovsky V L 2002 *Phys. Rev.* B **66** 014414
[25] Bergeret F S, Efetov K B and Larkin A I 2000 *Phys. Rev.* B **62** 11872
[26] Aladyshkin A Yu, Mel'nikov A S and Ryzhov D A 2003 *J. Phys.: Condens. Matter* **15** 6591
[27] Misko V R, Fomin V M, Devreese J T and Moshchalkov V V 2003 *Phys. Rev. Lett.* **90** 147003
[28] Milosevic M V and Peeters F M 2005 *J. Low Temp. Phys.* **139** 257
[29] Berthod C 2005 *Phys. Rev.* B **71** 134513
[30] See for instance Halterman K and Valls O T 2001 *Phys. Rev.* B **65** 014509